Evolution of Surface Functional Groups in a Series of Progressively Oxidized Graphite Oxides

Tamás Szabó,[†,‡] Ottó Berkesi,[§] Péter Forgó,[∥] Katalin Josepovits,[⊥] Yiannis Sanakis,[⊗] Dimitris Petridis,[⊗] and Imre Dékány[*,†,○]

Department of Colloid Chemistry, Department of Physical Chemistry, Department of Organic Chemistry, and Nanostructured Materials Research Group of the Hungarian Academy of Sciences, University of Szeged, H-6720 Szeged, Hungary, Department of Atomic Physics, Budapest University of Technology and Economics, H-1521 Budapest, Hungary, and Institute of Materials Science, NCSR "DEMOKRITOS", GR-15310 Athens, Greece

Received February 2, 2006. Revised Manuscript Received March 29, 2006

This study contributes to the sustained effort to unravel the chemical structure of graphite oxide (GO) by proposing a model based on elemental analysis, transmission electron microscopy, X-ray diffraction, ^{13}C magic-angle spinning NMR, diffuse reflectance infrared Fourier transform spectroscopy, X-ray photoelectron spectroscopy, and electron spin resonance investigations. The model exhibits a carbon network consisting of two kinds of regions (of trans linked cyclohexane chairs and ribbons of flat hexagons with C═C double bonds) and functional groups such as tertiary OH, 1,3-ether, ketone, quinone, and phenol (aromatic diol). The latter species give clear explanation for the observed planar acidity of GO, which could not be interpreted by the previous models. The above methods also confirmed the evolution of the surface functional groups upon successive oxidation steps.

Introduction

Among the colloidal forms of carbonaceous materials, there is a graphite-derived compound with layered structure, graphite oxide (GO), that has drawn less attention despite its prominent properties. Surfactant-intercalated GO may be used as a host material for molecular recognition.[1,2] Exfoliated GO/polymer nanocomposites are precursors for the preparation of conductive composites[3,4] and ultrathin carbon films;[5−7] attempts for microfabrication of carbonaceous electronic circuits from GO have been reported recently.[8] Microporous, SiO_2-pillared carbon adsorbents with high surface area[9,10] and stable aqueous dispersions of nanosized graphitic platelets[11] were also prepared via heat treatment or reduction of exfoliated GO. Potential benefits of oxidized graphites are still not exhausted with these: any other applications can be envisioned in principle that demand "forcing graphite skeleton into water", that is, that require hydrophilic, delaminated carbonaceous sheets.

It is clear that knowledge of the surface chemistry of GO is inevitable if our aim is to exploit this substance efficiently for the above-mentioned purposes. Yet, although GO was first prepared just 150 years ago,[12] its exact chemical structure is still ambiguous. Although GO has been extensively studied by X-ray diffraction (XRD), the wealth of data on layer distances contrasts starkly with the paucity of information on crystallographic parameters. The structure analysis is difficult also because (i) GO is a nonstoichiometric compound with a variety of compositions depending on the synthesis conditions, (ii) it is strongly hygroscopic, and (iii) it slowly decomposes above 60−80 °C. There is even no consensus to answer the question whether the hexagonal graphite lattice and the planarity of the carbon layers are fully conserved in this compound. Originally, Hofmann and Holst[13] proposed that the oxygen was bound to the carbon atoms of the hexagon layer planes by epoxy (1,2-ether) linkages with an ideal formula of C_2O (Scheme 1). In the Ruess model[14] a wrinkled carbon sheet composed of trans linked cyclohexane chairs is assumed, and the fourth valencies of carbon atoms are bound to axial OH groups and ether oxygens in 1,3 positions. This model is the first to account for the hydrogen content of GO which was supplemented with C═C double bonds, ketone, and enolic groups by Clauss and co-workers.[15] They also explained the observed acidity by enolic OH species along the layer planes,

* To whom correspondence should be addressed. Phone: +36-62-544210. Fax: +36-62-544042. E-mail: i.dekany@chem.u-szeged.hu.
† Department of Colloid Chemistry, University of Szeged.
‡ Current address: Centrum voor Oppervlaktechemie en Katalyse, K.U. Leuven, B-3001 Leuven, Belgium.
§ Department of Physical Chemistry, University of Szeged.
∥ Department of Organic Chemistry, University of Szeged.
⊥ Department of Atomic Physics, Budapest University of Technology and Economics.
⊗ Institute of Materials Science, NCSR "DEMOKRITOS".
○ Nanostructured Materials Research Group of the Hungarian Academy of Sciences, University of Szeged.

(1) Matsuo, Y.; Hatase, K.; Sugie, Y. *Chem. Lett.* **1999**, *28*, 1109.
(2) Matsuo, Y.; Niwa, T.; Sugie, Y. *Carbon* **1999**, *37*, 897.
(3) Du, X. S.; Xiao, M.; Meng, Y. Z.; Hay, A. S. *Synth. Met.* **2004**, *143*, 129.
(4) Wang, G.; Yang, Z.; Li, X.; Li, C. *Carbon* **2005**, *43*, 2564.
(5) Kotov, N. A.; Dékány, I.; Fendler, J. H. *Adv. Mater.* **1996**, *8*, 637.
(6) Kovtyukhova, N. I.; Ollivier, P. J.; Martin, B. R.; Mallouk, T. E.; Chizhik, S. A.; Buzaneva, E. V.; Gorchinskiy, A. D. *Chem. Mater.* **1999**, *11*, 771.
(7) Szabó, T.; Szeri, A.; Dékány, I. *Carbon* **2005**, *43*, 87.
(8) Hirata, M.; Gotou, T.; Ohba, M. *Carbon* **2005**, *43*, 503.
(9) Wang, Z.-M.; Hoshinoo, K.; Shishibori, K.; Kanoh, H.; Ooi, K. *Chem. Mater.* **2003**, *15*, 2926.
(10) Bourlinos, A. B.; Gournis, D.; Petridis, D.; Szabó, T.; Szeri, A.; Dékány, I. *Langmuir* **2003**, *19*, 6050.
(11) Stankovich, S.; Piner, R. D.; Chen, X.; Wu, N.; Nguyen, S. T.; Ruoff, R. S. *J. Mater. Chem.* **2006**, *16*, 155.
(12) Brodie, B. *Ann. Chim. Phys.* **1855**, *45*, 351.
(13) Hofmann, U.; Holst, R. *Ber. Dtsch. Chem. Ges.* **1939**, *72*, 754.
(14) Ruess, G. *Monatsch. Chem.* **1946**, *76*, 381.

10.1021/cm060258+ CCC: $33.50
Published on Web 05/04/2006

Scheme 1. Previous Structure Models of GO

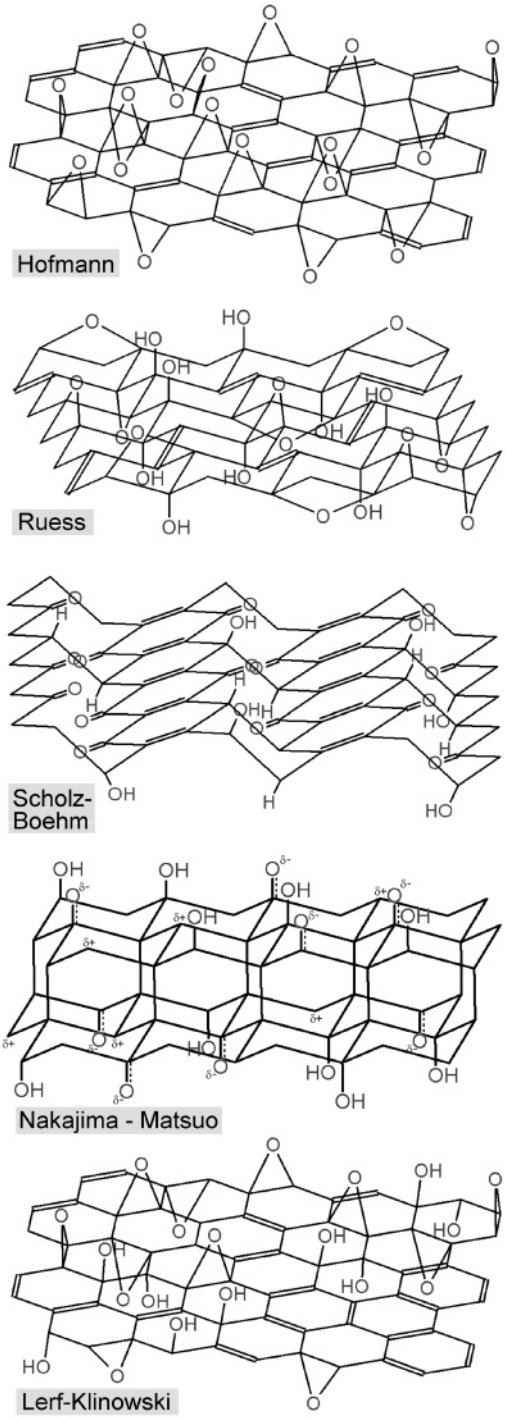

together with the existence of carboxylic groups around the edges of the lamellae. After stereochemical reconsiderations, this model was revised by Scholz and Boehm:[16] GO is characterized by the lack of ether oxygen and presence of corrugated carbon layers consisting of linked ribbons with rigid quinoidal structure. Later, Mermoux et al.[17] supported the Ruess model by proposing a structure analogous to that of poly(carbon monofluoride), $(CF)_n$. On the contrary, Nakajima et al.[18,19] proposed a stage 2 type $(C_2F)_n$ model by fluorination of GO. Recently, Cataldo has reviewed the structural analogies and differences between GO and polymeric fullerene oxides,[20] and the development of the oxygenated groups during the synthesis process has been studied by Hontoria-Lucas et al.[21] Yet all the previous models were supplanted by that proposed by Lerf and co-workers.[22−24] This model, based on expert NMR studies, depicts a GO layer as a random distribution of flat aromatic regions with unoxidized benzene rings and wrinkled regions of alicyclic six-membered rings bearing C═C, C−OH, and ether groups (reassigned to 1,2 positions), and the sheets of GO terminate with C−OH and COOH groups.

In the present paper the chemistry of surface functional groups of GO and its evolution during oxidation are scrutinized by the most relevant characterization techniques, and a model exhibiting some new structural features is proposed.

Experimental Section

Synthesis of GOs. The GOs were prepared from natural flaky graphite (99.98 wt % C; Graphitwerk Kropfmühl AG, Germany) based on the Brodie method.[12] The crude graphite (G) was sieved, and the portion within the size range of 250−500 μm was used. Graphite (10 g) and $NaClO_3$ (85 g) were mixed in a round flask placed into an ice bath. Next, 60 mL of fuming HNO_3 was added from a dropping funnel in 210 min. The obtained dark green thick slurry, containing the first stage graphite intercalation compound (graphite nitrate), was left aging at ambient temperature (18 h). The loss of HNO_3 due to evaporation was retrieved by adding another portion of acid (40 mL). The slurry was then heated to 60 °C with a steam bath and kept strictly at 60 ± 1 °C for 8 h. The heating rate (<1.5 °C/min) was controlled carefully to avoid dangerous deflagration. The reaction was terminated by transferring the pasty mixture into 1 L of distilled water. The diluted suspension was washed with 5 × 200 mL of 3 M HCl solution and at least with 7 × 1 L of distilled water to remove acidic and saline impurities until the supernatant had an electrical conductivity less than 10 μS/cm (very close to that of distilled water). The residual GO was separated by sedimentation and finally dried at 60 °C. This first specimen of the GO series (GO-1) was oxidized by (to GO-2) applying exactly the same procedure and quantity of ingredients, except a triple quantity (30 g) of GO-1 was used instead of graphite. Then, the whole oxidation procedure was repeated twice more to obtain the most oxidized graphites. The four samples will be denoted henceforth as GO-1, GO-2, GO-3, and GO-4 where 1−4 refer to the number of progressive oxidation steps.

Characterization of GOs. Transmission electron microscopy (TEM) images were taken on a Philips CM-10 electron microscope operating at a 100 kV accelerating voltage. GOs were dispersed in dilute NaOH (pH 9−10) while graphite was sonicated in a 50% (v/v) EtOH/water mixture to partly exfoliate. Aliquots from the supernatants were dropped on Formvar coated copper grids.

XRD measurements were performed on a Philips PW 1830 diffractometer operating with a Cu anode (40 kV voltage, 30 mA cathodic current). Cu Kβ radiation was absorbed by a Ni filter.

(15) Clauss, A.; Plass, R.; Boehm, H.-P.; Hofmann, U. *Z. Anorg. Allg. Chem.* **1957**, *291*, 205.
(16) Scholz, W.; Boehm, H.-P. *Z. Anorg. Allg. Chem.* **1969**, *369*, 327.
(17) Mermoux, M.; Chabre, Y.; Rousseau, A. *Carbon* **1991**, *29*, 469.
(18) Nakajima, T.; Mabuchi, A.; Hagiwara, R. *Carbon* **1988**, *26*, 357.
(19) Nakajima, T.; Matsuo, Y. *Carbon* **1994**, *32*, 469.
(20) Cataldo, F. *Fullerenes, Nanotubes, Carbon Nanostruct.* **2003**, *11*, 1.
(21) Hontoria-Lucas, C.; López-Peinado, A. J.; López-González, J. D.; Rojas-Cervantes, M. L.; Martín-Aranda, R. M. *Carbon* **1995**, *33*, 1585.
(22) He, H.; Riedl, T.; Lerf, A.; Klinowski, J. *J. Phys. Chem.* **1996**, *100*, 19954.
(23) Lerf, A.; He, H.; Riedl, T.; Forster, M.; Klinowski, J. *Solid State Ionics* **1997**, *101−103*, 857.
(24) Lerf, A.; He, H.; Forster, M.; Klinowski, J. *J. Phys. Chem. B* **1998**, *102*, 4477.

Table 1. Colors, Empirical Chemical Formulas, C/O Ratios, Water Contents, and XRD Parameters of the GO Series[a]

sample	color	chemical formula	C/O	H_2O content (wt %)	2Θ (deg)	d_{002} (nm)
graphite	grey	C		0	26.28	0.339
GO-1	grey	$C_2O_{0.77}H_{0.29}$	2.60	7.7	12.82	0.691
GO-2	gold	$C_2O_{0.90}H_{0.35}$	2.22	10.0	12.76	0.694
GO-3	orange	$C_2O_{0.92}H_{0.39}$	2.17	10.4	12.76	0.694
GO-4	brown	$C_2O_{0.98}H_{0.40}$	2.04	11.2	12.72	0.696

[a] All data refer to samples equilibrated with 70% relative humidity except for the water content (50% relative humidity) and chemical formulas, which correspond to anhydrous GOs.

Elemental analysis was carried out by a Perkin-Elmer 2400 series I. CHNS/O analyzer.

For ^{13}C magic-angle spinning (MAS) NMR measurements, a Bruker Avance DRX500 spectrometer was used operating in a 11.7 T magnetic field (^{13}C, 125.7 MHz) equipped with a 4 mm diameter solid-state probe head. ZrO_2 rotors were used with an approximately 100 mg amount of GO samples rotating at a 5 kHz speed. Tetramethylsilane was used as the external reference material ($\delta = 0$ ppm for ^{13}C). ^{13}C MAS NMR spectra were recorded with 4 μs excitation pulses and applying interpulse delays of 5 s. The detected spectral width was 300 ppm in all cases, and the carrier frequency was placed at 110 ppm. A total of 2K transients were recorded in 4K complex datapoints resulting in a 27.3 ms long acquisition time. A 50 Hz Lorentzian window function was applied prior to the Fourier transformation.

Infrared spectra were collected by using a Biorad FTS-60A FT-IR device equipped with a diffuse reflectance unit. A total of 10.0 $\pm$ 0.1 mg of GO was mixed with 320 $\pm$ 0.3 mg of finely ground KBr and placed in the sample holder of the reflection unit which was then purged for at least 20 min by a continuous flow of dry air before each measurement. For deuteration experiments, the spectrometer and the desiccator containing anhydrous GO/KBr mixtures were set under a drybox in which all the experimental procedures (desiccator opening, sample preparation, and its attachment to the reflection unit) were performed. The drybox was flushed with dry air for 12 h prior to collecting the spectrum. Then, anhydrous GOs were placed back into the desiccator containing D_2O (100.0%, Aldrich) for 7 days. The drybox technique was applied again to protect the deuterated GOs from changing back with water molecules. The diffuse reflectance infrared Fourier transform (DRIFT) spectra were recorded by a DTGS detector from 256 scans in a digital resolution of 2 cm^{-1}.

X-ray photoelectron spectra of GOs were obtained by using an XR3E2 (VG Microtech) twin anode X-ray source and a Clam2 hemispherical electron energy analyzer. The used Mg Kα radiation (1253.6 eV) was non-monochromatized. Survey scan spectra in the 1000−0 eV binding energy range were recorded with a pass energy of 50 eV. High-resolution spectra of the C 1s signals were recorded in 0.05 eV steps with a pass energy of 20 eV. After the linear baseline was subtracted, the curve fitting was performed by a mixed Gaussian−Lorentzian product function (30% Gaussian contribution).

Electron spin resonance (ESR) measurements were carried out at room temperature by a Bruker ER200D instrument equipped with an Anristsu microwave counter. The power and frequency of the microwave radiation were 34 mW and 9.41 GHz, respectively.

Results

Evidences for the Formation of GOs. The first oxidative treatment of graphite afforded the GO-1 sample with dark gray color very similar to the parent graphite (Table 1). The subsequent oxidation steps, though, yielded light brown/orange solids, as generally reported for well oxidized GOs.[15,16] This suggests that the oxidation is incomplete after the first step and crystalline graphite residues remain in the solid product. On the other hand, no phase separation of graphite traces was observed after having suspended GO-1 in dilute alkaline solutions, and the finely dispersed GO kept its dark gray color, suggesting that even the first treatment produced a uniform GO phase. To overcome this contradiction, the oxidation of graphite was studied by electron microscopy, XRD, and elemental analysis.

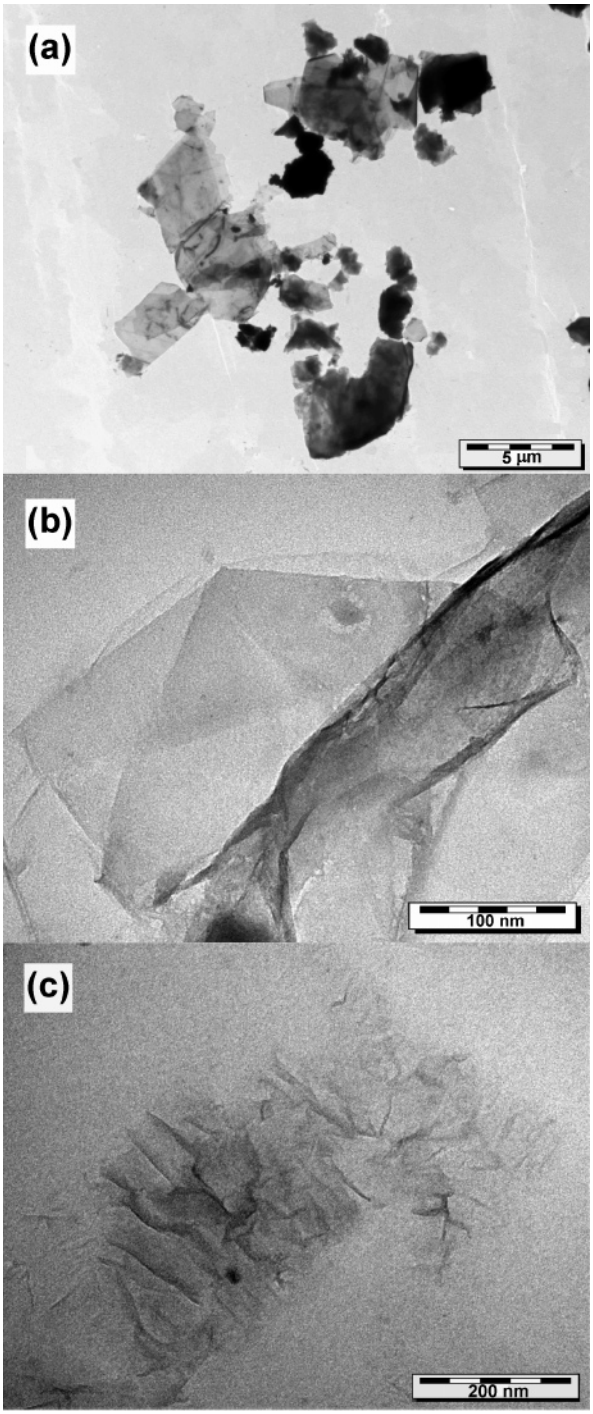

Figure 1. TEM images of (a) graphite, (b) GO-1, and (c) GO-4.

Electron Microscopy. TEM images of graphite, GO-1, and GO-4 are presented in Figure 1a−c, respectively. Graphite crystallites are micrometer-sized and appear as

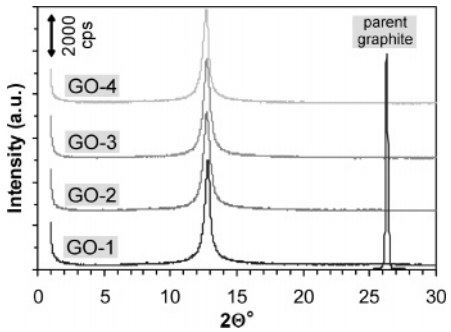

Figure 2. XRD patterns of GOs and their parent graphite. Curves of GOs are offset by 2500 cps (counts per second).

relatively thick, stacked aggregates of graphenes. The oxidized samples have two remarkably different microstructural features. First, the graphite particles are delaminated to very thin GO membranes with much smaller lateral dimensions than the coarse aggregates. Even the images of the black GO-1 sample showed only a very few areas resembling the original graphite slabs. Second, the oxides are no longer totally flat and smooth but always exhibit some folding. The crumpled sheets are very similar to those observed earlier for pure[25] and reduced[26] GO. Especially the GO-4 specimen shows considerable folding, which is not confined to any particular area of the particle. This suggests that the extent of folding increases with the degree of oxidation.

XRD. XRD provides conclusive proof for the completion of the oxidation reaction as the layer distances of the starting graphite and the end products are highly different (Figure 2). The diffractogram of graphite shows a very intense and narrow peak referring to X-ray reflection on the (002) planes of well-ordered graphenes. The basal spacing of air-dry GOs (equilibrated at 70% relative humidity) increases from 0.339 nm to 0.691−0.696 nm in the course of oxidation due to the expansion of the layer planes caused by the accommodation of various oxygen species. The XRD pattern of GO-1 features no reflection at $2\Theta = 26.28°$ that would indicate the abundance of unoxidized graphite residues. However, XRD is often just fairly sensitive to strong reflections. Therefore, we determined the detecion limit of our specific graphite sample in a powder mixture of the most highly oxidized, light brown GO-4. The peak at 26.28° could be detected even from a mixture of 0.1% graphite and 99.9% GO-4, meaning that the amount of intact graphite crystallites in GO-1 must be lower than 0.1% too, an amount which would certainly not be high enough to explain the very dark color of the moderately oxidized GO-1.

Study of the hydration behavior (water content and uptake rate) of GO was found to be crucial for the correct evaluation of the atomic composition and the interpretation of IR spectra. The GO samples were dried in a desiccator over concentrated H_2SO_4/silica gel for 1 month. These specimens will be denoted as anhydrous GOs. The XRD pattern of anhydrous GO-1 was recorded after opening the desiccator and covering the sample holder with Mylar foil immediately to prevent the adsorption of humidity. The foil was then removed, and XRD measurements were performed in the course of hydration to the air-dry state equilibrated at 50 ± 2% relative humidity. Figure 3a shows that anhydrous GO-1 has one reflection with basal spacing of 5.97 Å, one of the lowest values ever reported for dried GOs. Upon aging in a humid atmosphere, this reflection ($2\Theta = 14.85°$) lost intensity until fading into the background scattering. Simultaneously, a shoulder appeared at lower diffraction angles developing into a new peak corresponding to a higher basal spacing of air-dry GO-1 ($d_{002} = 6.30$ Å). The existence of two distinct peaks in the partially hydrated samples indicates a discontinuous increment in basal spacing from the dehydrated to the air-dry state due to the incorporation of H_2O molecules into the interlamellar space. Because anhydrous GO shows only the higher angle reflection, intercalated water content is effectively removed after the prolonged drying process. The water content and the kinetics of hydration were determined by mass measurements. Figure 3b shows the mass increase of anhydrous GO-1 upon exposure to a humid (50%) atmosphere, as well as the intensities of hydrated GO reflections. Adsorption of H_2O vapors was found to be rapid during the first minutes, though the equilibrium was reached after about 3 h. The more oxidized GOs take up the water in a shorter time (curves not shown), and their water content is higher that that of GO-1 (see Table 1), indicating that the highly oxidized samples are more hydrophilic.

Elemental Analysis. GOs consist of carbon, oxygen, and hydrogen. The atomic composition of a specific sample was found to vary with the synthetic methods and conditions (time and temperature oxidation) and the origin and grain size of

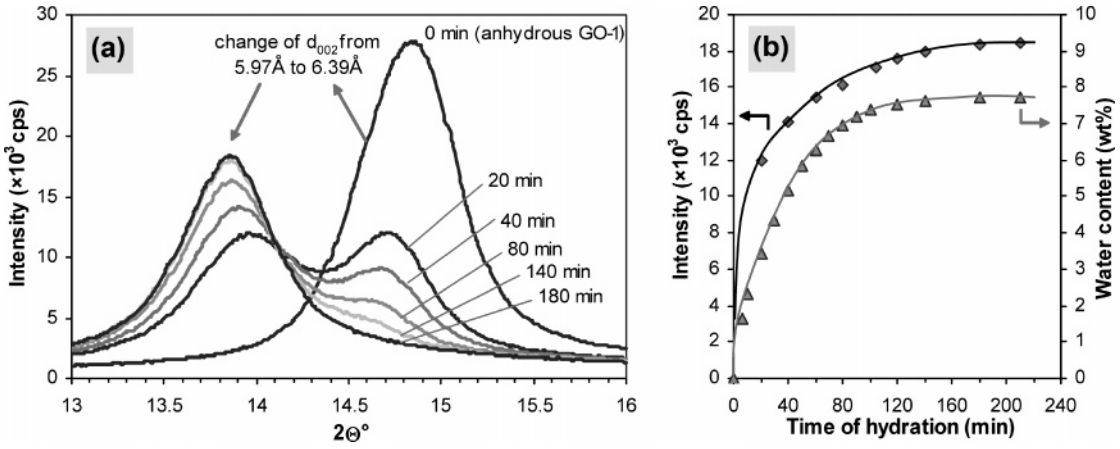

Figure 3. XRD patterns (a) and water uptake curves (b) of anhydrous GO-1 exposed to air of 50% relative humidity.

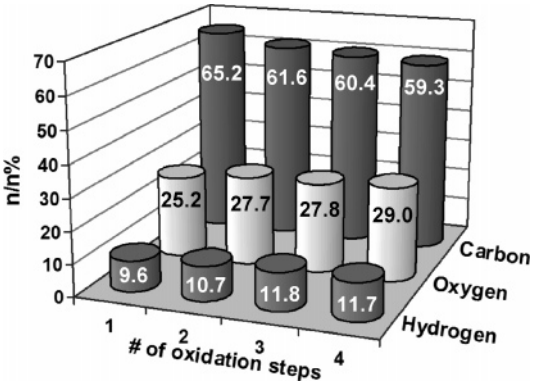

Figure 4. Atomic composition of anhydrous GOs.

the graphite specimen.[18,27] In addition, we observed that slow decomposition of fuming HNO_3 (in several months) greatly impoverished the efficiency of oxidation, resulting in less or incompletely oxidized graphite. Scholz and Boehm introduced the C/O ratio as a convenient measure of the oxidation degree of GOs.[16] As a result of the above reasons, this ratio was often reported to be significantly different; however, in most cases it ranges from about 1.8 to 2.5. The amounts of structural H atoms differ even more owing to the higher uncertainty in their determination, which is based on the small mass of H and the difficulties in producing and handling anhydrous samples. As revealed by XRD and mass measurements, water uptake is very fast, and thus weigh-in of anhydrous GO for elemental analysis is charged by considerable error. Therefore, we have performed the analysis on air-dry samples equilibrated at the same (50%) relative humidity as applied for hydration measurements, and thus the correct atomic compositions (Figure 4) and empirical chemical formulas (Table 1) for anhydrous GOs can be calculated as well. The oxygen and hydrogen content of GO increases with the degree of oxidation, with a concomitant decrease in the carbon content and the C/O ratio. The differences are relatively high between GO-1 and GO-2. The C content differs by 3.45 wt % (=3.6%, mol/mol). This value is too high to account for graphite residues because, as shown by XRD, their amount must be less than 0.1 wt %. Thus, elemental analysis also supports that the moderately oxidized GO-1 sample contains one phase, and all of its carbon atoms belong to the GO structure. Further oxidation results in a less pronounced change between members of the GO series. For GO-4, the C/O ratio approaches a value of 2, allowing a chemical formula of $C_2OH_{0.4}$ (or $C_{10}O_5H_2$) for the fully oxidized GO to be given.

Analysis of Functional Groups by Spectroscopic Methods

^{13}C MAS NMR. The spectra of different GO samples exhibit similar resonance patterns featuring five peaks (Figure 5). In contrast to the NMR results of Hontoria-Lucas et al.[21] their relative intensities did not change significantly upon oxidation. The signal at 69.2 ppm is unambigusly assigned to C—OH groups, while aromatic functionalities and/or conjugated double bonds resonate at 128.2 ppm.[9,17,21−24] The most intense peak, appearing at 57.6 ppm, was first attributed to 1,3 ethers,[17] reassigned later by Klinowski et al. to epoxides (i.e., 1,2-ethers).[22−24] The origins of the peaks at 92.9 and 166.3 ppm are not clearly revealed; however, the latter is strongly supposed to indicate the presence of C=O species. A slight peak at similar chemical shifts was only obseved before by Wang and co-workers in the case of bare GO,[9] although the resonances of carbonyl groups in a maleic acid derivative of GO were also assigned to 170 ppm.[24]

DRIFT Spectroscopy. GO received close scrutiny by infrared specroscopy. Despite some trivial band assigments, though, the elucidation of other peaks differs even among

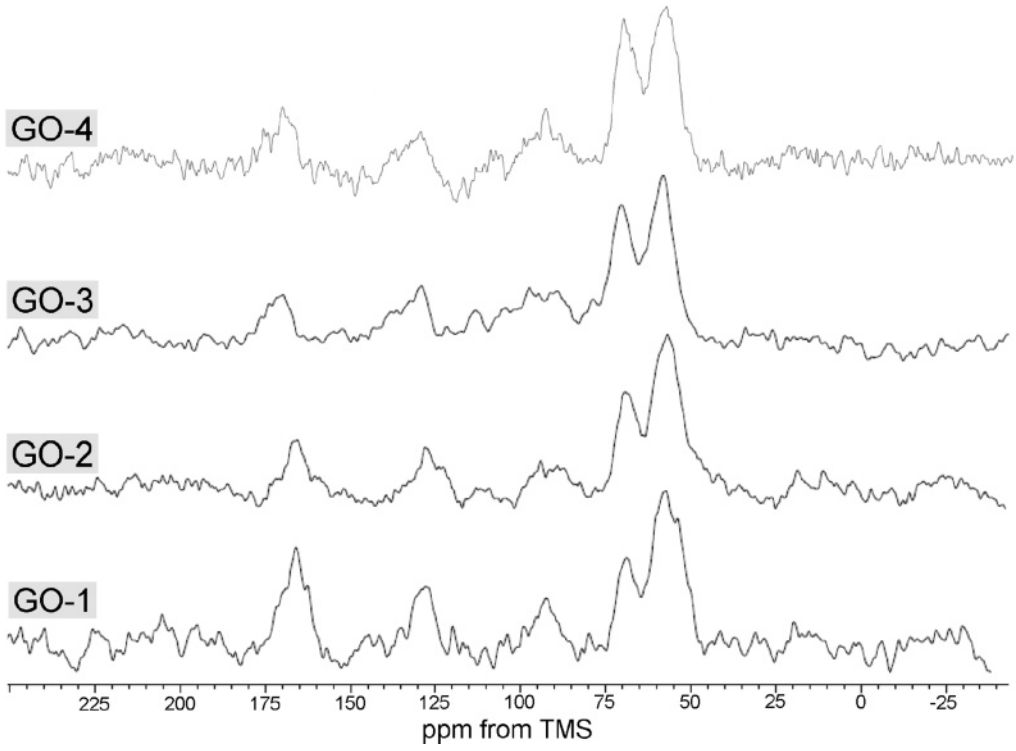

Figure 5. ^{13}C MAS NMR spectra of the GO series.

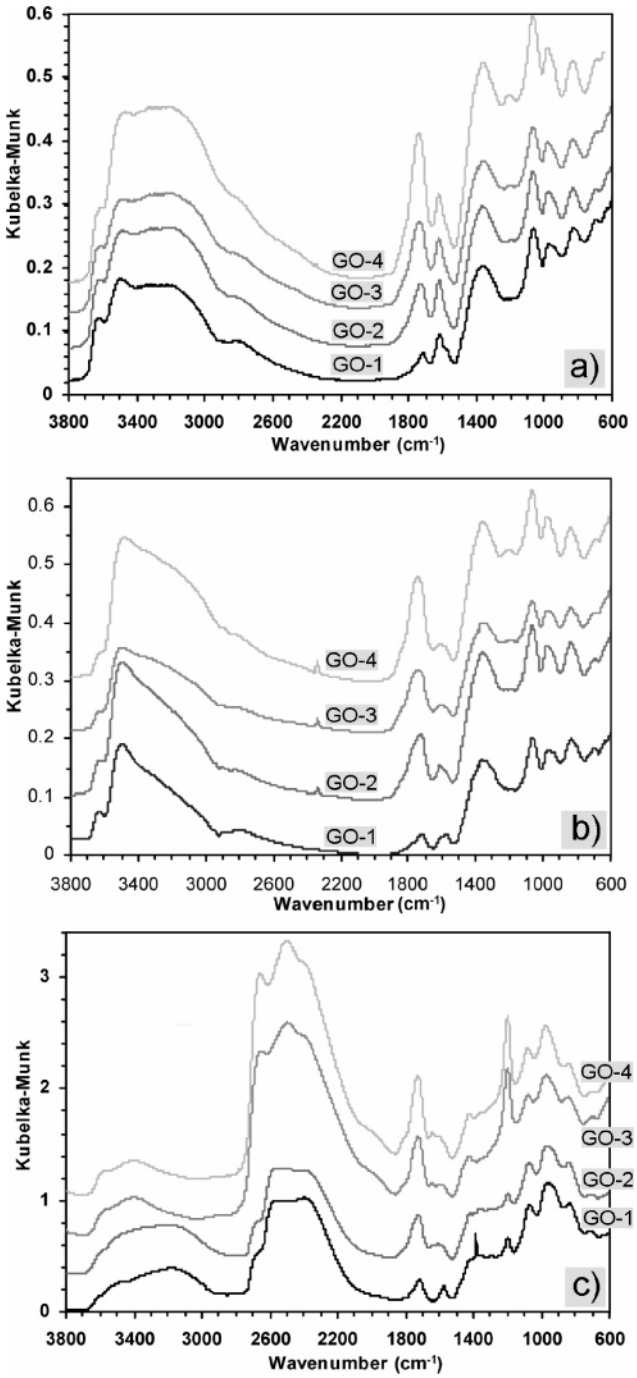

Figure 6. DRIFT spectra of (a) air-dry GOs, (b) anhydrous GOs, and (c) deuterium-exchanged GOs. For clarity, all related curves are offset by the same Kubelka−Munk units. Part a reprinted with permission from ref 38. Copyright 2006 Elsevier Sci., Ltd.

the recent IR studies. The reason is the high and strongly bound humidity content of GO which may result in a misleading interpretation of the spectrum, and the broad and strong OH bands may obscure or totally cover other peaks as well. According to our perusal of the literature, no special attempts have been exercised for the removal of the physically adsorbed water during IR measurements. Application of dry atmosphere or degassing prior to recording the spectrum is inadequate as dehydration requires much more time, that is, at least several weeks. Heating is also not viable because GO is thermally unstable. The OH peaks, however, can be eliminated by deuterium exchange as demonstrated for GO-1 in our recent paper,[28] which we extend here to the GO series.

Table 2. IR Peak Positions (in cm^{-1}) of Air-Dry GO-1 ($GO\text{-}1/H_2O$), GO-4 ($GO\text{-}4/H_2O$), and Deuterated GO-1 ($GO\text{-}1/D_2O$) and Their Assignments[a]

$GO\text{-}1/H_2O$	$GO\text{-}4/H_2O$	$GO\text{-}1/D_2O$	assignment
		3210 m, br	ν_{OH} in HDO
3630* m, sp	3634* w, sh	2680* m, sh	ν_{OH} in C−OH/ν_{OD} in C−OD
3490* s, sp	3490* m, sp	2568* vs, br	ν_{OH} in C−OH/ν_{OD} in C−OD
3210* s, br	3190* s, br	2396* vs, br	ν_{OH} in H_2O/ν_{OD} in D_2O
2814 w, br	2780 w, sh		ν_{OH} in dimeric COOH
1714 m, sp	1738 vs, sp	1716 m, sp	$\nu_{C=O}$
1616* m, sp	1616* s, sp	1196* m, sp	β_{OH} in H_2O/β_{OD} in D_2O
1574 w, sh		1574 m, sp	aromatic $\nu_{C=C}$
1368* s, br	1370* s, br	968* s, br	β_{OH} in C−OH/β_{OD} in C−OD
		1384 m, sp	organic carbonate
	1196		phenolic OH
1064 968 828 698	1066 978 828 696	1064 968 828 698	skeletal modes of ν_{C-C} and ν_{C-O} bonds (*m, sp*)

[a] Asterisks (in the same row) designate isotopomer peak pairs. Band intensities and widths are classified as w (weak), m (medium), s (strong), vs (very strong), sh (shoulder), sp (sharp), and br (broad).

The spectrum of air-dry GO-1 (Figure 6a) exhibits overlapping bands in the 3800−2200 cm^{-1} range corresponding to the stretching vibrations of structural OH groups and physisorbed water molecules (peak positions are given in Table 2). No clear distinction seems possible between C−OH and H_2O peaks. The next, relatively strong band (at 1714 cm^{-1}) is most often related to the C═O stretching of COOH groups situated at the edges of the oxidized graphenes. In our recent study[28] we have shown that functional groups other than COOH, anhydride, or lactone (the latter two, via alkaline hydrolysis, would give carboxylates as well) must also feature the GO structure that gives the $\nu_{C=O}$ signal which strongly suggests the presence of single ketones or quinones. Another controversial assignment corresponds to the peak located near 1620 cm^{-1}. It was attributed either to oxygen surface compounds, like cyclic ethers, or to ring vibrations throughout the carbon skeleton,[29] but the HOH bending vibrations also appear in a very close range of wavenumbers. The shoulder at 1574 cm^{-1} (see also Figure 7a) may reflect the presence of unoxidized aromatic regions of GO-1, although hydrogen bonding and cooperative effects may result in a large dispersion of β_{OH} wavenumbers, and the shoulder could also refer to OH vibration. Finally, bending of tertiary C−OH groups (1368 cm^{-1}) and the fingerprint region, composed of C−O and C−C stretching combinations, characterize the spectrum of air-dry GO-1. There are prominent changes in the spectra of the highly oxidized, air-

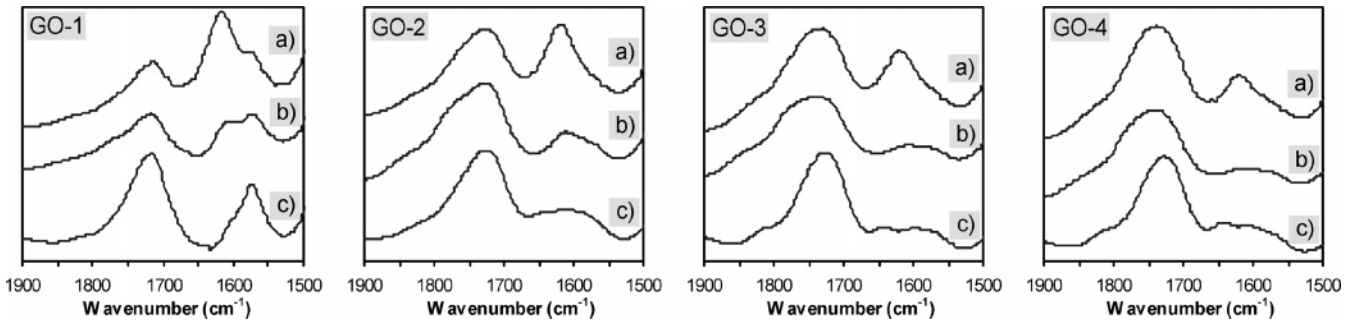

Figure 7. 1900−1500 cm^{-1} region of (a) air-dry GO, (b) anhydrous GO, and (c) deuterated GO DRIFT spectra. The ordinate scale is arbitrary.

dry GOs as compared to GO-1. First, the infrared absorption of the OH stretching vibrations, along with that of HOH bending, is getting higher and higher upon oxidation, without a concomitant increase of the β_{C-OH} peak at 1368 cm^{-1}. This finding points out that the highly oxidized GO surfaces are more hydrophilic (in agreement with the hydration experiments) that is, conversely, not attributed to the increase of C—OH groups. Instead, it is due to the development of carbonyl groups on the surface as indicated by the huge intensity increase of the $\nu_{C=O}$ peak (which gradually overtakes the neighboring water band). Another important difference between spectra of GO-1 and those of other GOs is that the latter do not feature the shoulder at 1574 cm^{-1} (Figure 7a), which is likely due to the destruction of aromatic regions at a high degree of oxidation. Finally, the appearance of a new band at 1200 cm^{-1} is clearly observed, especially for GO-4, which is ascribed to phenolic groups giving an IR signal in this region. Such species have been postulated to decorate, along with COOH groups, the zigzag edges of GO sheets. A recent quantum chemical study of carbon model compounds[29] has shown, though, that such terminal OH groups, via cooperative effects, induce ring vibrations around 1600 cm^{-1} and a strong IR absorption in the 1420−1480 cm^{-1} region. Because GO spectra exhibit no peaks in the latter range, we suggest the presence of phenolic moieties in the "bulk" of the carbon network and not, or not exclusively, on the edge sites.

Drying over H_2SO_4 affects the intensities of the broad band series between 3700 and 2200 cm^{-1} and the peak at 1616 cm^{-1} as shown by the spectra in Figure 6b. The two ν_{OH} band components of higher wavenumbers (3630 and 3490 cm^{-1}) must refer to structural OH groups as their shape remains unchanged after drying. On the other hand, the 3210 cm^{-1} peak loses intensity; thus, we assign it as a water OH peak. The same happens with the β_{HOH} band near 1620 cm^{-1} (Figure 7b). Because these water related peaks do not disappear, it is likely that water traces still remain in the solid. As shown by XRD, anhydrous GO-1 does not contain water in the interlamellar space, so these H_2O molecules must be situated near the edges of the layers and/or condensed in the small voids and pores of the solid.[30] Another interesting finding (in the case of GO-1) is the transformation of the original shoulder-like band structure to two peaks near 1600 cm^{-1} which, close to the HOH bending peak, suggests the presence of a $\nu_{C=C}$ skeletal band of aromatic domains.

Deuterium exchange on GOs manifests in the shifting toward lower frequencies of all peaks related to vibrational modes contributed by the internal coordinates of the OH unit (Figure 6c). The OH/OD isotopomer peak pairs can be clearly assigned as the ratio of their wavenumbers shows excellent agreement with the theoretically predicted value of $2^{-1/2}$.[28] The appearance of the broad band series between 2700 and 1900 cm^{-1}, the peak at 1200 cm^{-1}, and the enhanced absorption in the fingerprint region (968 cm^{-1} peak) are all related to the H to D exchange. On the other hand, the β_{OH} peak of C—OH species disappears, indicating that all the hydrogen atoms are replaced from the structural hydroxyl groups. Consequently, the OH stretching peaks of C—OH must be missing from the spectrum, which is true for the peaks at 3630 and 3490 cm^{-1}. Therefore, deuteration makes possible the distinction between ν_{OH} of structural hydroxyl groups and adsorbed water. The broad band centered at 3210 cm^{-1} retained in the spectrum of D_2O exchanged GOs is characteristic for the HDO vibrations,[31] clearly indicating that this peak corresponded originally (in air-dry GO) to water molecules.[32] Figure 7c shows the effect of deuteration on the band around 1600 cm^{-1}. In contrast to air-dry and anhydrous GO spectra, there are no band components at 1616 cm^{-1}. This finding indicates not only that there are no H_2O molecules in D_2O exchanged GO but also that there are no or very few functional groups (e.g., pyrone moieties) in the GO structure that could promote IR absorption at this wavenumber, and originally, in the air-dry GO, only the water molecules were responsible for the signal. Lack of any strong peaks after deuteration also supports our previous suggestion about the formation of phenolic groups over the basal planes of GO. Finally, the hydroxyl β_{OH} to β_{OD} band shift reveals a very sharp peak at 1384 cm^{-1} covered in the air-dry GO-1, most probably originating from organic carbonates.[28] As this peak does not appear in the case of the

(25) Beckett, R. J.; Croft, R. C. *J. Phys. Chem.* **1952**, *56*, 929.
(26) Boehm, H.-P.; Clauss, A.; Fischer, G. O.; Hofmann, U. *Z. Naturforsch.* **1962**, *17*, 150.
(27) Boehm, H.-P.; Scholz, W. *Liebigs Ann. Chem.* **1966**, *691*, 1.
(28) Szabó, T.; Berkesi, O.; Dékány, I. *Carbon* **2005**, *43*, 3186.
(29) Fuente, E.; Menéndez, J. A.; Díez, M. A.; Suárez, D.; Montes-Morán, M. A. *J. Phys. Chem. B* **2003**, *107*, 6350.
(30) It is noteworthy that, because the mesoporosity of GOs is very low, the amount of water in the dried GOs is insignificant, causing negligible error in the determination of chemical formulae.
(31) Nakamoto, K. *Infrared and Raman spectra of inorganic and coordination compounds*, 5th ed.; Wiley: New York, 1997.
(32) Existence of HDO molecules is expected because, after exchange of the hydrogen content of anhydrous GO in a high excess of ambient D_2O molecules, H must be present as HDO instead of H_2O due to entropy effects.

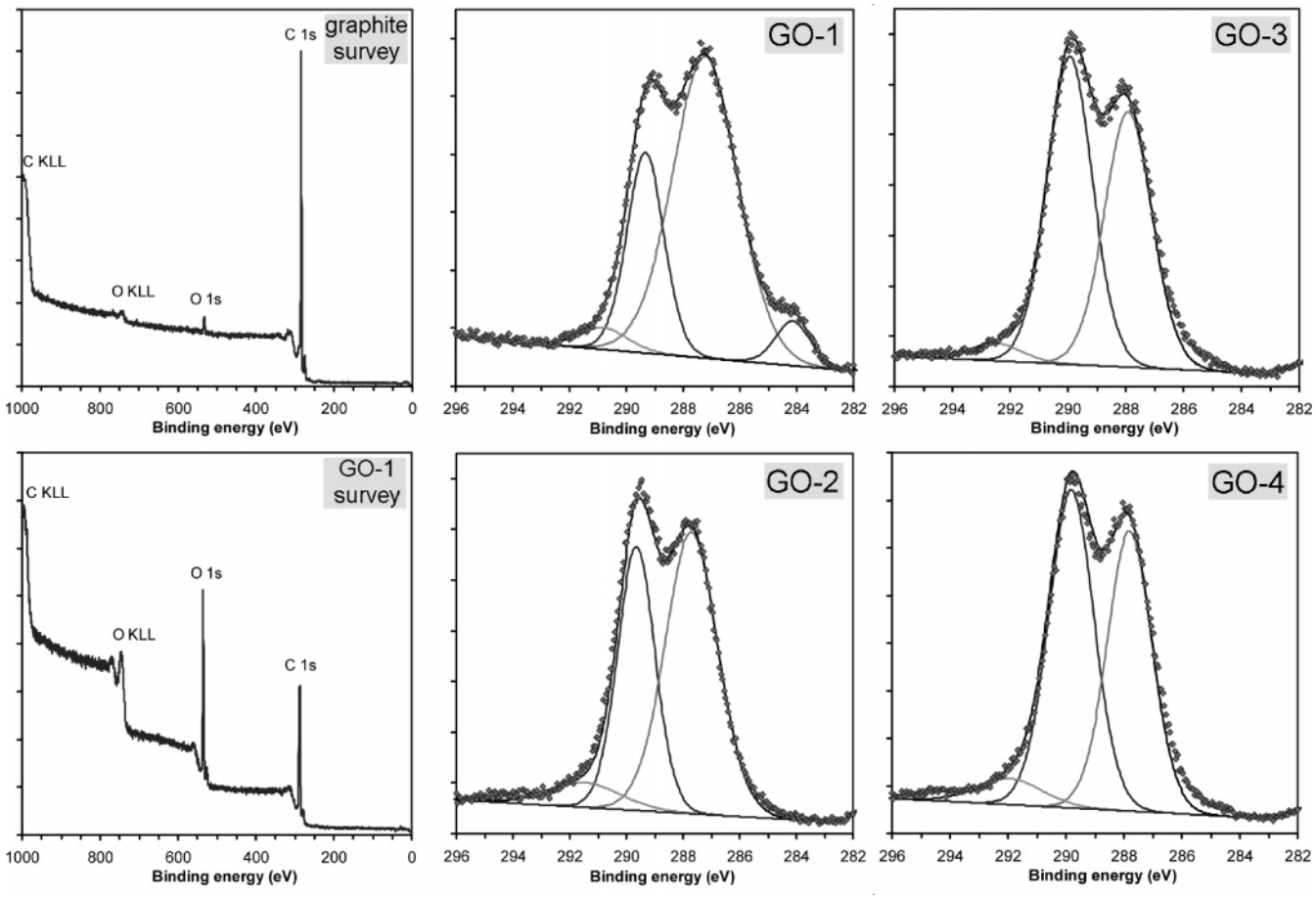

Figure 8. Survey scan and high-resolution XPS spectra of graphite and derived GOs.

highly oxidized samples, this species is just an intermediate product in the formation process of GO.

X-ray Photoelectron Spectroscopy. Figure 8 shows the XPS spectra of the bare graphite and the GO series. The survey scan spectra indicate the presence of C and O atoms at the surface of both solids. The oxygen content of GOs is much higher because of the oxidative treatment, while for graphite it is explained by a slight atmospheric oxidation.[33] The C 1s region of the graphite spectrum (not shown) exhibits only one asymmetric peak, centered at 284.1 eV, tailing on the high-energy side due to the π-bond shake-up satellite.[34,35] The signal of graphitic materials is found at 284.4 eV in the literature.[36] It suggests the existence of a systematic error in our case, shifting all peak positions by −0.3 eV. The sign of this shift is negative; thus, it cannot originate from the charging effect. We must stress, though, that this slight deviation does not change the conclusions that can be obtained about the structure of GO from our XPS measurements. The high-resolution XPS spectra of GOs show several relatively well-resolved peaks corresponding to carbon atoms in different chemical environments. Summing peaks from four (for GO-1) or three types of carbons on the

Table 3. XPS Data of the C 1s Envelope of GOs Deconvoluted into Four Peaks: Area Percentages and Binding Energies (in Parentheses)

sample	peak 1, % (eV)	peak 2, % (eV)	peak 3, % (eV)	peak 4, % (eV)
GO-1	5.3 (284.1)	66.3 (287.2)	24.9 (289.3)	3.5 (290.8)
GO-2		56.0 (287.7)	37.3 (289.6)	6.7 (291.5)
GO-3		45.1 (287.9)	51.7 (289.9)	3.2 (292.5)
GO-4		43.7 (287.8)	50.3 (289.8)	6.0 (291.9)

experimental data (represented by dots) gave an excellent fit. Table 3 shows the binding energies and the corresponding area percentages of the deconvoluted C 1s envelopes. The first peak of GO-1 has the same position as that of graphite, indicating the presence of aromatic carbon atoms in this sample and that the charging effect during the measurement was successfully avoided as well. The other three Gaussian peaks are considered to originate from C atoms bound with one, two, and three valencies to O atoms, because electronegative oxygen induces a partial positive charge on the carbon atom. Thus, we assign the peak at 287.2 eV to alcohols, phenols, and ethers, at 289.3 eV to ketones, and at 290.8 eV to carboxylic groups, respectively. The chemical shifts of these satellites are rather high. For example, a bonding energy of 289.3 eV is generally attributed to COOH groups instead of C═O. In this case, however, it is not possible because the area of this peak is about 25%; that is, every fourth carbon atom should be present as a carboxylic group, which would be too high even for the smallest, nanometric GO sheets that possess a relatively high amount of edge sites. Instead, the high chemical shifts can be

(33) Kinoshita, K. *Carbon, electrochemical and physicochemical properties*; Wiley: New York, 1988.
(34) Kovtyukhova, N. I.; Mallouk, T. E.; Pan, L.; Dickey, E. C. *J. Am. Chem. Soc.* **2003**, *125*, 9761.
(35) Ago, H.; Kugler, T.; Cacialli, F.; Salaneck, W. R.; Shaffer, M. S. P.; Windle, A. H.; Friend, R. H. *J. Phys. Chem. B* **1999**, *103*, 8116.
(36) Davis, D. W.; Shirley, D. A. *J. Electron Spectrosc. Relat. Phenom.* **1974**, *3*, 137.

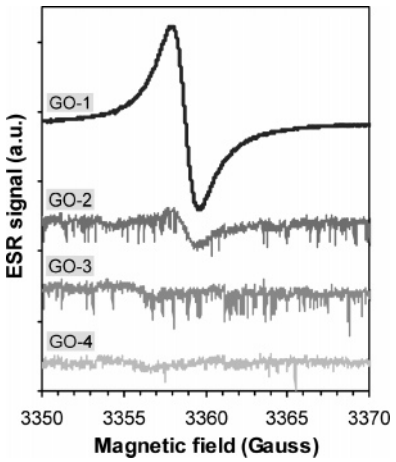

Figure 9. ESR spectra of GOs. Signal intensity of GO-1 is reduced by one magnitude.

explained by GOs being much richer in oxygen than other carbon materials, and the electron withdrawing effect of the large number of heteroatoms adjacent to a C atom is more pronounced.

The changes observed in the spectra of the other GO samples clearly correlate with the degree of oxidation. The 284.1 eV peak disappears, owing to the loss of aromaticity in well-oxidized GOs. The binding energies of the satellites slightly shift toward higher values because the well-oxidized samples are much less conductive than GO-1, resulting in charging of the samples while recording the spectra. The C 1s envelope changes shape also because the peak of the ketones is gradually overtaking (both in intensity and area) that at 287.2 eV. This suggests, in agreement with the chemical formulas and C/O of the GO series, that the average oxidation degree of carbon atoms increases with the number of successive chemical treatments, which is due to the disappearance of unoxidized aromatic domains over the carbon network, and that some surface species (e.g., alcohols or ethers) oxidize further to ketones or carboxylic groups.

ESR Spectroscopy. To the best of our knowledge, no studies have been conducted yet to investigate the ESR of GO. However, the line shapes, widths, and intensities of carbon materials are affected by chemical treatment, and the electron spins are sensitive probes of their microscopic environment.[33] Strong ESR in graphite is known to be due to conduction electrons, while many amorphous carbons, such as carbon blacks, exhibit only a weak, broad signal or no resonance at all. According to Figure 9, GO-1 shows a sharp and intensive derivative peak. The small width of this peak implies that there are no conduction carriers in this solid like in graphite, that is, there are no highly extended aromatic sheets that would develop a conduction band. Instead, the origin of the spin species may be either free radicals probably associated with the broken bonds at edge sites/defects or, as suggested by Collins et al.,[37] mobile π electrons that are stabilized by the resonance energy in the condensed aromatic ring structure. This issue can be decided by considering the spectra of the other samples: the signal can hardly be observed for GO-2, while GO-3 and GO-4 show no resonance. The disappearance of the peak clearly proves that originally, in GO-1, it was given by aromatic areas because if free radicals also contributed then the signal should not disapperar after the subsequent oxidation steps, but even a higher amount of broken bonds would be expected to be created. Therefore, ESR affords final conclusive evidence that GO-1 does not contain intact graphenes or graphite crystals, and even the first oxidation yields a uniform GO phase containing condensed polyaromatic domains of nanometric or sub-nanometric dimensions over its lamellae.

(37) Collins, R. L.; Bell, M. D.; Kraus, G. *J. Appl. Phys.* **1959**, *30*, 56.

Table 4. Merits and Drawbacks of the Previous and the New Structure Models

characteristics	Hofmann	Ruess	Scholz−Boehm	Nakajima−Matsuo	Lerf−Klinowski	new model
chemical formula	−	+	+	+	+	+
lack of highly distorted or instable structure elements	+	−	+	−	+	+
IR spectrum	−	−	−	+	−	+
XPS spectrum	−	−	+	−	−	+
planar acidity	−	−	+	−	−	+

Discussion

The results of the above analytical techniques clearly point out that the previous structural models of GO (Scheme 1) cannot be upheld in every respect because all of them feature several structural characteristics that cannot be reconciled with the observed properties of GO. These drawbacks are summarized in Table 4, where "+" and "−" represent whether the model in question satisfies (+) the given chemical property or not (−). These issues are as follows:

1. The Hofmann model contains no H atoms, which inevitably exist in GO.

2. The Ruess model does not count for C═O groups, and the formation of double bonds between tetrahedrally coordinated (sp^3) carbon atoms should be highly disadvantageous, if it exists at all.

3. Instable structure elements are also involved in the Nakajima−Matsuo model, which contains quasi-pentacovalent carbon (i.e., carbonyl groups holding partial negative charges are supposed to bound to three other carbon atoms). We think that carbocation-like species featuring the model cannot exist; for example, they should readily react with the adjacent axial $C{=}O^{\delta-}$ species to form 1,3-ethers. On the other hand, the stage-2 type carbon skeleton, which they assume on the basis of fluorination of GO, is a remarkable feature of their model.

4. The Lerf−Klinowski model assumes C═O species existing only in COOH groups at the edge sites of GO sheets. However, the high area of the C═O satellite in the XPS spectra as well as the lack of carboxylate peaks in the IR spectrum of the Na salt of GO proves that a considerable amount of C═O moieties such as ketones and/or quinones are present on the basal planes of GO.

5. The Scholz and Boehm model is the only one explaining the planar acidity of GO, which we observed by potentio-

Scheme 2. New Structure Model of GO: (a) Surface Species and (b) Folded Carbon Skeleton

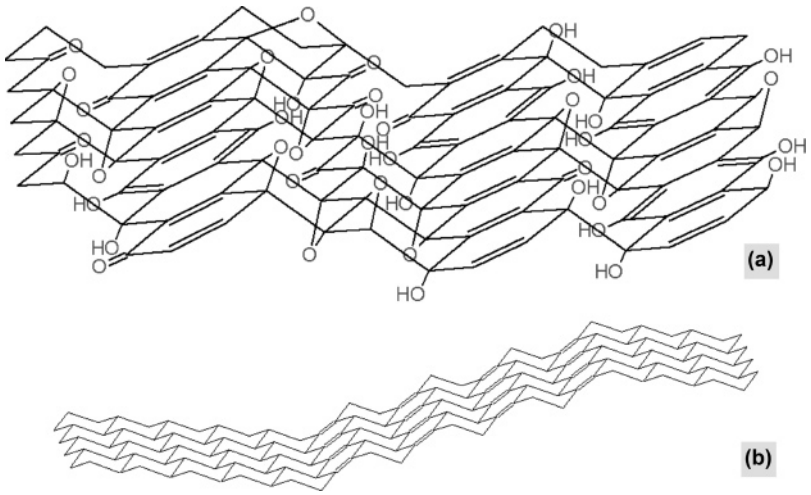

metric acid−base titrations,[38] but it is also supported by numerous XRD studies that indicated the presence of (acidic) cation-exchange sites in the interlamellar space. They assumed a keto/enol tautomerism in GO, and the enol form affords the acidic sites. Yet, it is known that normally the tautomer equilibrium highly tends toward the keto form, and they could not account for any structure elements that would cause favorable enolization. Another problem raised was that the model involved C−H bonds, which should have appeared in the IR spectrum.

New Structure Model. For the structural description of GO, we have revived the model of Scholz et al. applying some modifications so that it should explain all the experimental results obtained. The model, depicted in Scheme 2a, has a corrugated carbon network including a ribbonlike arrangement of flat carbon hexagons connected by C=C double bonds. These ribbons are linked together to a two-dimensional frame by periodically cleaved ribbon(s) of cyclohexane chairs. While Scholz et al. proposed that the hexagons were connected directly (forming thus a ribbon as wide as one chair), our model shows that it is possible to extend the lateral dimension of the cyclohexane network. Hence, the resulting carbon skeleton is a mixture of the Ruess and Scholz−Boehm skeleton, including a random distribution of two kinds of domains: that of the trans linked cyclohexane chairs and that of the corrugated hexagon ribbons. There is a slight tilting angle between the boundary of these regions (Scheme 2b) which may explain the wrinkling of the layers observed by TEM. In case of moderate oxidation, GO contains condensed aromatic rings confined to small (nanometric) areas, which disappear in highly oxidized samples. The surface species are tertiary OH groups and 1,3-ethers lying above and below the cyclohexane sheets, while cyclic ketones and quinones can be formed on the hexagon ribbons where the C−C bonds are cleaved. Furthermore, it is also possible to include phenolic groups into the bulk of the layers, by which the planar acidity can be easily explained without assuming instable enols and C−H bonds in GO. The total amount of oxygen-containing groups increases upon progressive oxidation with a concomitant change in the surface speciation; for example, organic carbonates are just intermediate products, while others like OH and 1,3-ether groups may oxidize further to ketones, or part of the carbon double bonds may also be oxygenated (to epoxides or vicinal diols).

Acknowledgment. The present publication was supported by the Innovation Fund of Science and Research and the GSRT in the frame of a Greek-Hungarian Intergovernmental Science & Technology cooperation. The authors thank Dr. Aristides Bakandritsos from IMS Demokritos for his assistance with the ESR measurements and Professor Hanns-Peter Boehm for helpful correspondence.

CM060258+

(38) Szabó, T.; Tombácz, E.; Illés, E.; Dékány, I. *Carbon* **2006**, *44*, 537.